

# Mott transition from the non-analyticity of the one-body reduced density-matrix functional

Zhengqian Cheng and Chris A. Marianetti

*Department of Applied Physics and Applied Mathematics, Columbia University, New York, NY 10027*

(Dated: August 21, 2025)

One-body reduced density-matrix functional (1RDMF) theory has yielded promising results for small systems such as molecules, but has not addressed quantum phase transitions such as the Mott transition. Here we explicitly execute the constrained search within a variational ansatz to construct a 1RDMF for the multi-orbital Hubbard model with up to seven orbitals in the thermodynamic limit. The variational ansatz is the  $\mathcal{N} = 3$  ansatz of the variational discrete action theory (VDAT), which can be exactly evaluated in  $d = \infty$ . The resulting 1RDMF exactly encapsulates the  $\mathcal{N} = 3$  VDAT results, which accurately captures Mott and Hund physics. We find that non-analytic behavior emerges in our 1RDMF at fixed integer filling, which gives rise to the Mott transition. We explain this behavior by separating the constrained search into multiple stages, illustrating how a nonzero Hund exchange drives the continuous Mott transition to become first-order. Our approach creates a new path forward for constructing an accurate 1RDMF for strongly correlated electron materials.

One-body reduced density matrix functional (1RDMF) theory can be viewed as a formalism to encapsulate the ground state properties for a class of Hamiltonians with fixed interactions and arbitrary one-body terms [1–5]. There have been successes in developing explicit interaction energy functionals which produce reasonable energetics in various molecules [5–11] and single orbital Hubbard models [12–22], in addition to select observables in crystals [23–27]. However, there has not been a rigorous demonstration that any existing 1RDMF can capture the Mott transition. Our focus is capturing local Mott and Hund physics, which is hosted in strongly correlated electron materials (SCEM) which often bear  $d$  or  $f$  electrons [28]. The essence of SCEM is embodied by the multi-orbital Hubbard model in infinite dimensions, which facilitates numerically exact solutions and serves as a reasonable starting approximation for crystals in two and three dimensions [28–31]. A robust 1RDMF of the multi-orbital Hubbard model should satisfy the following criteria, which are dictated by numerically exact solutions in infinite dimensions. First, the Mott transition must be predicted at a finite Hubbard  $U$ . Second, the order of the Mott transition must be properly predicted with or without the Hund coupling  $J$ . Third, the aforementioned goals should be achieved while maintaining the symmetry of the Hamiltonian, proving that the functional can faithfully describe Mott and Hund physics. Here we demonstrate that an accurate 1RDMF that satisfies the preceding criteria can be constructed by *exactly* executing the constrained search within the  $\mathcal{N} = 3$  sequential product density matrix (SPD) ansatz of the variational discrete action theory (VDAT) in infinite dimensions [32, 33]. Given that VDAT at  $\mathcal{N} = 3$  has been demonstrated to accurately capture Mott and Hund physics [34, 35], the resulting 1RDMF serves as an efficient approach to exactly encapsulate VDAT results. A companion article to this Letter introduces the qubit parameterization of VDAT, which provides the technical

tools needed to execute the constrained search [36].

For simplicity, we consider the translationally invariant Hamiltonian  $\hat{H} = \sum_{k\ell} \epsilon_{k\ell} \hat{n}_{k\ell} + \hat{H}_{int}$ , where  $k$  labels a reciprocal lattice point,  $\ell$  enumerates  $2N_{orb}$  spin orbitals, and the interaction Hamiltonian is  $\hat{H}_{int} = \sum_i H_{loc}(\{\hat{n}_{i\ell}\})$  where  $H_{loc}$  is an arbitrary polynomial function and  $\hat{n}_{i\ell}$  is the density operator for spin orbital  $\ell$  at site  $i$ . It should be noted that the one-body contribution is restricted to be diagonal in  $\ell$ , which is a common simplification used when studying the multi-orbital Hubbard model (e.g. see Ref. [37]). For this class of Hamiltonians, the interaction energy functional is defined as

$$E_{int}(\{n_{k\ell}\}) = \frac{1}{L} \min_{|\Psi\rangle} \left\{ \langle \Psi | \hat{H}_{int} | \Psi \rangle \mid \langle \Psi | \hat{n}_{k\ell} | \Psi \rangle = n_{k\ell} \right\}, \quad (1)$$

where  $|\Psi\rangle$  is a normalized state in the many-particle Fock space,  $L$  is the number of sites in the lattice, and  $n_{k\ell} \in [0, 1]$ . For a given  $\hat{H}_{int}$ , the interaction functional  $E_{int}$  is universal in the sense that it provides the ground state energy for Hamiltonians with arbitrary  $\epsilon_{k\ell}$  as follows

$$E = \min_{\{n_{k\ell}\}} \left( \frac{1}{L} \sum_{k\ell} \epsilon_{k\ell} n_{k\ell} + E_{int}(\{n_{k\ell}\}) \right). \quad (2)$$

While  $E_{int}(\{n_{k\ell}\})$  must be explicitly constructed for a given  $\hat{H}_{int}$ , the interacting energy functional for  $\lambda \hat{H}_{int}$ , where  $\lambda$  is a positive number, is the interacting energy functional for  $\hat{H}_{int}$  multiplied by  $\lambda$ .

We begin by examining the fidelity of numerous explicit 1RDMF's from the literature by applying them to the single-orbital Hubbard model in  $d = \infty$ , including the MBB [38], CA [39], CGA [40], and power [24] functionals, all of which approximate the interaction energy functional as a Hartree term plus an exchange-correlation term which consists of independent contributions from each spin orbital. We compare all functionals to numerically exact solutions obtained using dynamical mean-field

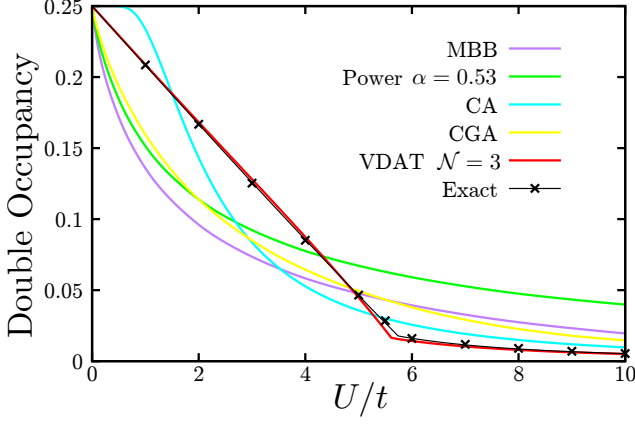


Figure 1. The double occupancy vs.  $U/t$  for the single-orbital Hubbard model on the Bethe lattice in  $d = \infty$  using four 1RDMF's: MBB, Power, CA, and CGA. The exact (DMFT) and VDAT results are taken from Ref. [32]. The black line is obtained from interpolations of the metallic and insulating DMFT data.

theory (DMFT) [29, 30] with the numerical renormalization group (NRG) impurity solver [41], in addition to VDAT results for  $\mathcal{N} = 3$  [32] (see Figure 1). The VDAT results correctly describe the continuous Mott transition [29], identified by a kink in the double occupancy at  $U/t = 5.61784$ , and accurately agree with the DMFT results. The MBB, CA, CGA, and power functionals are all substantially in error, and qualitatively fail to predict the Mott transition at a finite  $U/t$ . More advanced functionals, including PNOF5 [8] and PNOF7 [42], also perform poorly in the absence of symmetry breaking [36].

Our proposed solution for obtaining the interaction energy functional is to rigorously execute the constrained search within the sequential product density matrix (SPD) ansatz [32, 33], which is the ansatz used in VDAT. The variational freedom of the SPD is set by an integer  $\mathcal{N}$ , where  $\mathcal{N} \rightarrow \infty$  encapsulates the exact solution, and there are two types of SPD: G-type or B-type. A restricted form of the SPD has been evaluated using quantum Monte-Carlo to solve the single-orbital Hubbard model in two dimensions [43–48], the  $p$ - $d$  model [49, 50], and selected molecules [51]. Alternatively, VDAT has been used to exactly evaluate the SPD in the Anderson impurity model [32], the single orbital Hubbard model in  $d = \infty$  [32], and the multi-orbital Hubbard model in  $d = \infty$  [34, 35]. Nonetheless, constructing  $E_{int}(\{n_{k\ell}\})$  from any non-trivial variational ansatz is still highly challenging as there must be some efficient means to constrain the variational parameters to a particular  $\{n_{k\ell}\}$  and minimize over the remaining degrees of freedom. The recently developed qubit parameterization of VDAT allows for the constrained search to be executed for the B-type  $\mathcal{N} = 2$  and the G-type  $\mathcal{N} = 2$  and  $\mathcal{N} = 3$  SPD,

and here we focus on G-type  $\mathcal{N} = 3$  (see Ref. [36] for  $\mathcal{N} = 2$ ).

We now proceed to construct the interaction energy functional via the  $\mathcal{N} = 3$  G-type SPD, and it is sufficient to restrict the SPD to a pure state which can be represented as

$$|\Psi\rangle = \exp\left(\sum_{k\ell} \gamma_{k\ell} \hat{n}_{k\ell}\right) \exp\left(\sum_{i\Gamma} v_{i\Gamma} \hat{X}_{i\Gamma}\right) |\Psi_0\rangle, \quad (3)$$

where  $|\Psi_0\rangle$  is a Slater determinant,  $\hat{X}_{i\Gamma}$  is a diagonal Hubbard operator at site  $i$ , and the variational parameters are  $\{\gamma_{k\ell}\}$ ,  $\{v_{i\Gamma}\}$ , and  $\{n_{k\ell;0}\}$ , where  $n_{k\ell;0} = \langle \Psi_0 | \hat{n}_{k\ell} | \Psi_0 \rangle \in [0, 1]$ . The index  $\Gamma$  enumerates all  $2^{2N_{orb}}$  local atomic states. The key idea is to reparametrize the variational parameters  $\{\gamma_{k\ell}\}$  and  $\{v_{i\Gamma}\}$  from Eq. 3 in terms of new variational parameters  $\{n_{k\ell}\}$  and  $\rho$ . The  $\{n_{k\ell}\}$  is the physical momentum density distribution taking values within  $[0, 1]$ , and has the same number of free parameters as  $\{\gamma_{k\ell}\}$ . The  $\rho$  is a many-body density matrix corresponding to a pure state of a  $2N_{orb}$  qubit system, which has the same number of independent parameters as  $\{v_{i\Gamma}\}$ . The qubit system is a convenient mathematical tool to represent local integer time correlation functions of the VDAT formalism as static observables [36]. There is a natural correspondence between the density operators in the local Fock space and the qubit space, where the local density operator is represented as  $\hat{n}_\ell = \frac{1}{2}(1 - \hat{\sigma}_\ell^z)$ , and  $\hat{\sigma}_\ell^\mu$  denotes the application of the  $\hat{\sigma}^\mu$  Pauli matrix to the  $\ell$ -th qubit subspace. Using these new variables, the interaction energy for a given set of variational parameters can be expressed as  $\langle \hat{H}_{eff} \rangle_\rho$ , where  $\hat{H}_{eff} = H_{loc}(\{\hat{n}_{eff,\ell}\})$  is defined in the qubit space, and  $\hat{n}_{eff,\ell}$  depends on the variational parameters only through the following five variables:  $n_\ell = \int dk n_{k\ell}$ ,  $\xi_\ell = \frac{1}{2} \langle \hat{\sigma}_\ell^x \rangle_\rho$ ,  $\Delta_\ell = \int_{>} dk n_{k\ell}$ , and  $\mathcal{A}_{X\ell} = \int_X dk \sqrt{n_{k\ell}(1 - n_{k\ell})}$ , where  $X$  takes two values denoted as  $<$  or  $>$  indicating that the integration is over the region where  $n_{k\ell,0} = 1$  or  $n_{k\ell,0} = 0$  for a given  $\ell$ , respectively. Here we have taken the continuum limit of the discretized  $n_{k\ell}$  and choose the convention  $\int dk = 1$ . It should be emphasized that  $\hat{n}_{eff,\ell}$  *analytically* depends on the preceding five variables (see Eq. 68 in Ref. [36]). Finally, the interaction energy functional can be conveniently expressed as a constrained minimization

$$E_{int}(\{n_{k\ell}\}) = \min_{\rho, \{n_{k\ell;0}\}} \langle \hat{H}_{eff} \rangle_\rho, \quad (4)$$

$$\text{subject to } \int dk n_{k\ell;0} = \left\langle \frac{1 - \hat{\sigma}_\ell^z}{2} \right\rangle_\rho = \int dk n_{k\ell}, \quad (5)$$

$$|\langle \hat{\sigma}_\ell^x \rangle_\rho| \leq 2\sqrt{(1 - n_\ell)n_\ell - (1 - \Delta_\ell)\Delta_\ell}, \quad (6)$$

which corresponds to an *exact* constrained search within the wave function given by Eq. 3 in  $d = \infty$ . We assume that the optimized  $n_{k\ell;0}$  is given as  $\theta(n_{k\ell} - n_\ell^*)$ ,

where  $\theta$  is the Heaviside function and  $n_\ell^*$  is chosen such that  $\int dk n_{k\ell;0} = n_\ell$ . The remaining challenge is how to efficiently minimize  $\langle \hat{H}_{eff} \rangle_\rho$  over  $\rho$ , which is non-trivial given that  $\hat{H}_{eff}$  depends on  $\rho$  through  $\xi_\ell$ . This challenge can be addressed by dividing the minimization into two stages. First,  $\{\xi_\ell\}$  can be fixed, which will fix  $\hat{H}_{eff}$ , and then  $\langle \hat{H}_{eff} \rangle_\rho$  can be minimized, which is equivalent to finding the ground state of  $\hat{H}_{eff} - \sum_\ell h_\ell^x \hat{\sigma}_\ell^x - \sum_\ell h_\ell^z \hat{\sigma}_\ell^z$ , where the Lagrange multipliers  $h_\ell^\mu$  are chosen to yield  $\langle \hat{\sigma}_\ell^x \rangle_\rho = 2\xi_\ell$  and  $\langle \hat{\sigma}_\ell^z \rangle_\rho = 1 - 2n_\ell$ . Second, the interaction energy functional is obtained by minimizing over  $\{\xi_\ell\}$ . In what follows, we will illustrate this two stage minimization for the case where  $n_{k\ell}$  is restricted to be independent of  $\ell$  and have particle-hole symmetry, which is sufficient to solve a multi-orbital Hubbard model where  $\epsilon_{k\ell}$  is independent of  $\ell$  and has particle-hole symmetry.

We consider the following multi-orbital interaction Hamiltonian  $H_{loc}(\{\hat{n}_\ell\}) = U\hat{O}$ , where

$$\hat{O} = \hat{O}_1 + \left(1 - 2\frac{J}{U}\right) \hat{O}_2 + \left(1 - 3\frac{J}{U}\right) \hat{O}_3, \quad (7)$$

where  $\hat{O}_1 = \sum_\alpha \delta \hat{n}_{\alpha\uparrow} \delta \hat{n}_{\alpha\downarrow}$ ,  $\hat{O}_2 = \sum_{\alpha<\beta,\sigma} \delta \hat{n}_{\alpha\sigma} \delta \hat{n}_{\beta\sigma}$ ,  $\hat{O}_3 = \sum_{\alpha<\beta,\sigma} \delta \hat{n}_{\alpha\sigma} \delta \hat{n}_{\beta\bar{\sigma}}$ , and  $\delta \hat{n}_{\alpha\sigma} = \hat{n}_{\alpha\sigma} - \frac{1}{2}$ , with the orbital indices  $\alpha, \beta$  taking values of  $1, \dots, N_{orb}$  and the spin index  $\sigma \in \{\uparrow, \downarrow\}$ . The restriction of particle-hole symmetry at half-filling ensures that  $\mathcal{A}_{<\ell} = \mathcal{A}_{>\ell}$  and  $n_\ell = \frac{1}{2}$ , and for convenience we define  $A = \mathcal{A}_{<\ell} + \mathcal{A}_{>\ell}$  and also discard the index  $\ell$  for  $\xi_\ell$  and  $\Delta_\ell$ . The interaction energy functional implicitly depends on  $N_{orb}$ ,  $U$ , and  $J$ , but scaling the interaction Hamiltonian will trivially scale the interaction energy functional. Therefore, the interaction energy functional only has a non-trivial dependence on  $N_{orb}$  and  $J/U$ .

The interaction energy per site can be written as  $\langle \hat{H}_{eff} \rangle_\rho = UA^4 \tilde{\mathcal{F}}^2(\Delta, \xi) \langle \hat{O} \rangle_\rho$  (see Eq. 431 in Ref. [36]), where

$$\tilde{\mathcal{F}}(\Delta, \xi) = \frac{2}{1 - 4\xi^2} \left( \sqrt{1 - \frac{4\xi^2}{(1 - 2\Delta)^2}} + 1 \right). \quad (8)$$

Following the two stage minimization outlined above, we first minimize the interaction energy over  $\rho$  under a constrained value of  $\xi$  by computing

$$\mathcal{O}(\xi) = \min_\rho \{ \langle \hat{O} \rangle_\rho \mid \frac{1}{2} \langle \hat{\sigma}_\ell^x \rangle_\rho = \xi, \langle \hat{\sigma}_\ell^z \rangle_\rho = 0 \}, \quad (9)$$

which encodes the essential information about all local correlations. The computational cost for evaluating  $\mathcal{O}(\xi)$  will generally scale exponentially in terms of  $N_{orb}$ , but it will be demonstrated that only a coarse discretization in  $\xi$  is needed to faithfully represent  $\mathcal{O}(\xi)$ . A given data point can be generated efficiently by solving the ground-state of  $\hat{O} - h \sum_\ell \hat{\sigma}_\ell^x$ , where  $h$  is a Lagrange multiplier, which is a transverse field Ising model. In Figure 2,  $\mathcal{O}(\xi)$

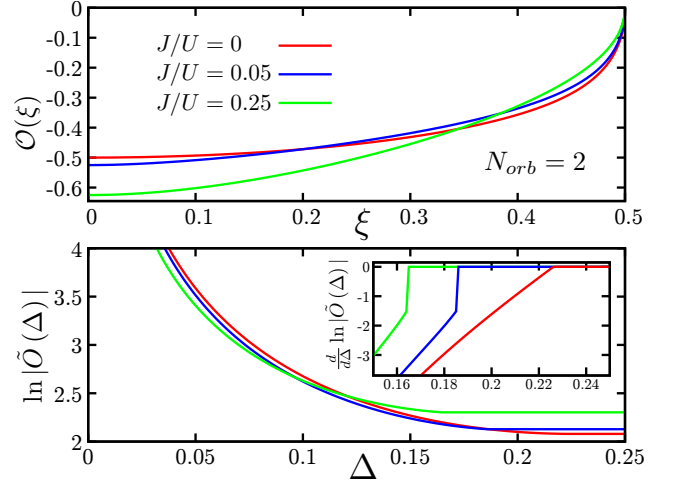


Figure 2. Plots of  $\mathcal{O}(\xi)$  (top) and  $\ln|\tilde{O}(\Delta)|$  (bottom) for  $N_{orb} = 2$  and various  $J/U$ ; the inset plots  $\frac{d}{d\Delta} \ln|\tilde{O}(\Delta)|$ , highlighting the non-analytic behavior in the 1RDMF.

is plotted for  $N_{orb} = 2$  and various  $J/U$ , demonstrating that the result is indeed a smooth function which can be accurately represented by a spline interpolation. Given that  $\mathcal{O}(\xi)$  is demonstrated to be an analytic function when  $|\xi| < \frac{1}{2}$ , any non-analytic behavior in the interaction energy functional must arise from minimizing over  $\xi$ . The interaction energy functional can be *explicitly* constructed when  $n_{k\ell}$  is independent of  $\ell$  and has particle hole symmetry, given as

$$E_{int}(\{n_{k\ell}\}) = UA^4 \tilde{O}(\Delta), \quad (10)$$

$$\tilde{O}(\Delta) = \min_{\xi \in [0, \frac{1}{2} - \Delta]} \tilde{\mathcal{F}}^2(\Delta, \xi) \mathcal{O}(\xi), \quad (11)$$

where  $\tilde{O}(\Delta)$  can be efficiently evaluated using the spline of  $\mathcal{O}(\xi)$ , and the result can be accurately represented with a spline interpolation as well. Moreover, for the case of  $N_{orb} = 1$ , an analytical form of  $\tilde{O}(\Delta)$  can be derived (see Eq. (103) in Ref. [36]). Given that  $\tilde{O}(\Delta)$  is constructed for a given  $J/U$  and  $N_{orb}$ , the result may be used to solve any model with  $\epsilon_{k\ell}$  independent of  $\ell$  with particle-hole symmetry and  $U$ . In Figure 2, we plot  $\ln|\tilde{O}(\Delta)|$  and  $d \ln|\tilde{O}(\Delta)|/d\Delta$  for  $N_{orb} = 2$  and various  $J/U$ , demonstrating that there is a discontinuity at  $\Delta = \Delta_c$  in the first derivative for  $J/U > 0$  and the second derivative for  $J/U = 0$ . The presence of non-analyticity in the interaction energy functional is profound, as it guarantees that there must be a phase transition for an arbitrary band structure at some critical  $U$ , and this transition will be demonstrated to be the Mott transition. This non-analytic behavior in the interaction energy functional should not be confused with the derivative discontinuity in density functional theory [52], which is associated with a change in the total number of particles and is present for all systems with a charge gap.

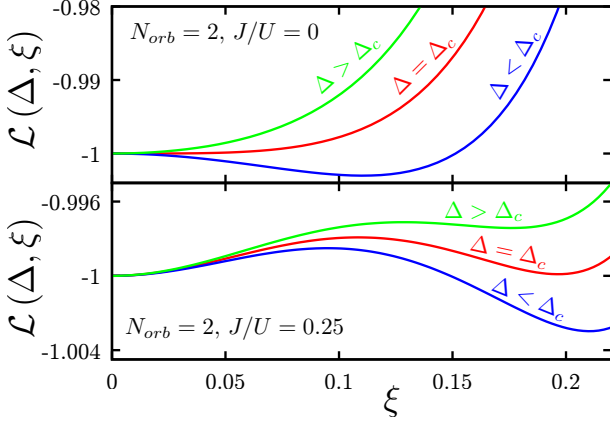


Figure 3. Graphical illustration of the origin of the non-analyticity in the interacting energy functional. Plots of  $\mathcal{L}(\Delta, \xi)$  versus  $\xi$  at  $N_{orb} = 2$  with  $J/U = 0$  (top) and  $J/U = 0.25$  (bottom) for various  $\Delta$ , where  $\Delta_c$  corresponds to the non-analytical point in  $\tilde{O}(\Delta)$ .

We now explore why  $E_{int}(\{n_{k\ell}\})$  has non-analytic regions by investigating the minimization over  $\xi$ . Consider the function  $\mathcal{L}(\Delta, \xi) = -\frac{\tilde{\mathcal{F}}^2(\Delta, \xi)\mathcal{O}(\xi)}{\tilde{\mathcal{F}}^2(\Delta, 0)\mathcal{O}(0)}$ , where  $\mathcal{L}(\Delta, 0) = -1$ . Finding the minimum of  $\mathcal{L}(\Delta, \xi)$  will yield the minimum of  $\tilde{\mathcal{F}}^2(\Delta, \xi)\mathcal{O}(\xi)$  used in Eq. 11, given that  $\tilde{\mathcal{F}}(\Delta, 0) = 4$  and  $\mathcal{O}(0) = -\frac{1}{4}N_{orb}(1 + (N_{orb} - 1)J/U)$ . We first consider  $J/U = 0$  at  $N_{orb} = 2$  for various  $\Delta$  (see Figure 3), demonstrating that the optimized  $\xi$  will continuously go to zero as  $\Delta$  increases through  $\Delta_c$ . Alternatively, for  $J/U > 0$ , the optimized  $\xi$  will discontinuously go to zero as  $\Delta$  increases through  $\Delta_c$ . Therefore, in both cases,  $\Delta > \Delta_c$  indicates  $\xi = 0$  and  $\frac{d\tilde{O}(\Delta)}{d\Delta} = 0$  (see Eq. 8), which can be seen in Figure 2. A sixth order Taylor series expansion of  $\mathcal{L}(\Delta, \xi)$  in terms of  $\xi$  can be used to provide an analytical understanding of the non-analyticity in  $\tilde{O}(\Delta)$  (see Section VII C in Ref. [36]).

We now demonstrate that  $\frac{d\tilde{O}(\Delta)}{d\Delta} = 0$  indicates that the system is in the Mott phase. Given that the interaction energy only depends on  $\{n_{k\ell}\}$  via  $\Delta$  and  $A$ , the total energy can be partially optimized for a fixed  $\Delta$  and  $A$ , which is achieved by the following momentum density distribution [35, 36]

$$n_{k\ell} = \frac{1}{2} \left( 1 - \frac{\text{sgn}(\epsilon_{k\ell})a + \epsilon_{k\ell}}{\sqrt{(\text{sgn}(\epsilon_{k\ell})a + \epsilon_{k\ell})^2 + b^2}} \right), \quad (12)$$

where  $a$  and  $b$  are Lagrange multipliers that are determined by  $\Delta$  and  $A$ . The partially optimized energy is a function of  $\Delta$  and  $A$ , and rewriting the saddle point equations yields  $a = \frac{UA^4}{4N_{orb}} \frac{d\tilde{O}(\Delta)}{d\Delta}$  and  $b = \frac{-2UA^3}{N_{orb}} \tilde{O}(\Delta)$  (see Eqns. (483) and (484) in Ref. [36]). Given that the quasiparticle weight  $Z = a/\sqrt{a^2 + b^2}$ , and that  $A > 0$  for finite  $U$ , the only scenario where  $Z = 0$  is when  $\frac{d\tilde{O}(\Delta)}{d\Delta} = 0$ . Determining the order of the phase tran-

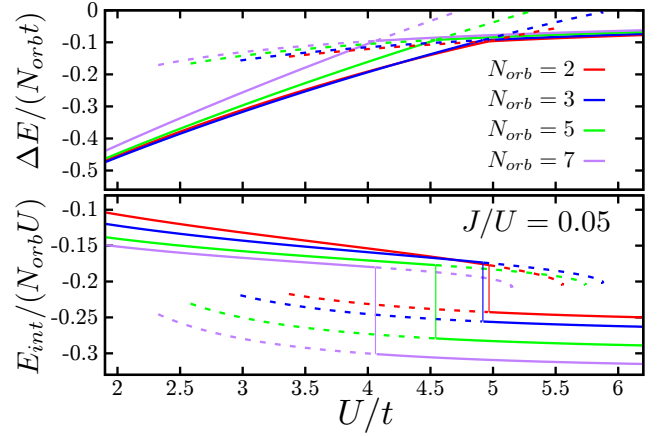


Figure 4. Plots of various energy contributions for the multi-orbital Hubbard model on the Bethe lattice in  $d = \infty$  for  $N_{orb} = 2, 3, 5, 7$  as a function of  $U/t$  for  $J/U = 0.05$ . (top) Plot of  $\Delta E/(N_{orb}t)$ , where  $\Delta E = E(U, J, t) - E(U, J, 0)$  and  $E(U, J, t)$  is the total energy per site. (bottom) Plot of  $E_{int}/(N_{orb}U)$ . The dotted lines indicate metastable solutions.

sition requires a global comparison of the total energy between the metal and insulating phases, and the transition only occurs at  $\Delta_c$  when the transition is continuous (see Section VII C in Ref. [36]).

We now proceed to use the 1RDMF to solve the multi-orbital Hubbard model on the Bethe lattice in  $d = \infty$  for  $N_{orb} = 2 - 7$ . While these results will be numerically identical to VDAT at  $\mathcal{N} = 3$  with a G-type SPD, the 1RDMF offers extraordinary practical advantages. The computational cost of the 1RDMF can be broken into two parts. First, the interaction energy functional must be constructed for a given  $N_{orb}$  and  $J/U$ , and the computational cost is dominated by the solution of a collection of quantum spin models with  $2N_{orb}$  spins. Second, the total energy must be minimized for a given Hamiltonian by solving the saddle point equations for  $a$  and  $b$ , which has a minimal cost. For a fixed  $J/U$  and  $N_{orb}$ , the interaction energy functional for arbitrary  $U$  can be obtained via scaling, allowing for the entire parameter space over  $U$  to be explored at a minimal computational cost. The total energy and the interaction energy are plotted as a function of  $U/t$  for  $J/U = 0.05$  and  $N_{orb} = 2, 3, 5, 7$  (see Figure 4). The dotted lines indicate a metastable metal or insulating phase. The Mott transition can be identified as a kink in the total energy or a discontinuity in the interaction energy, which is first-order in this case, consistent with previous Gutzwiller [53], slave boson [54], and DMFT [55] studies. Corresponding results for  $J/U = 0, 0.25$  are provided in Ref. [36]. Additionally, we explore how the Mott transition value  $U_c$  depends on  $N_{orb}$  for many different values of  $J/U$  (see Figure 5). For  $J/U = 0$ , we exactly recover the result from our previous VDAT study [35], which demonstrated excellent agreement with numerically exact DMFT solutions. For small

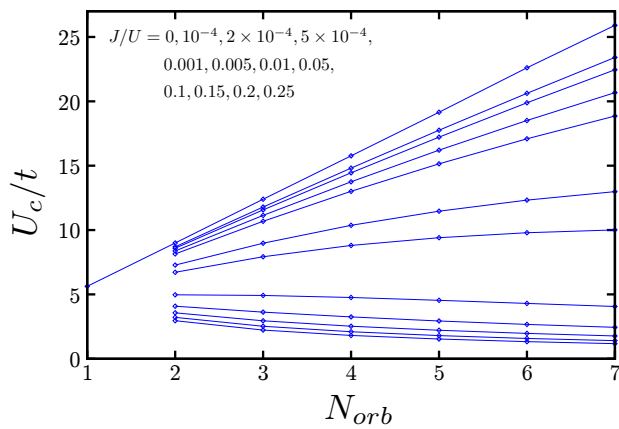


Figure 5. A plot of  $U_c$  for the multi-orbital Hubbard model on the Bethe lattice in  $d = \infty$  as a function of  $N_{orb}$  for various  $J/U$ , where  $U_c$  monotonically decreases with increasing  $J/U$  for a given  $N_{orb}$ .

$J/U$ , the  $U_c$  increases with  $N_{orb}$ , while the opposite happens for sufficiently large  $J/U$ . While previous DMFT studies already elucidated the fact that increasing  $J/U$  decreases  $U_c$  at a given  $N_{orb}$  for  $N_{orb} \leq 3$  [55–58], our results provide a clear understanding of how  $U_c$  depends on  $N_{orb}$  for a given  $J/U$  up to  $N_{orb} = 7$ .

In conclusion, we have provided a practical formalism for exactly executing the constrained search within the G-type  $\mathcal{N} = 3$  SPD in  $d = \infty$  to construct the 1RDMF for the multi-orbital Hubbard model. We explicitly illustrate that there is non-analyticity in the interaction energy functional for the multi-orbital Hubbard model which gives rise to the Mott transition and properly describes the order of the transition. While the Mott transition in  $d = \infty$  has been intensively studied, the 1RDMF demonstrates the universality of the Mott transition independent of the details of the band structure. Moreover, the 1RDMF is an efficient tool for accurately solving the ground state properties of the multi-orbital Hubbard model, yielding solutions for large  $N_{orb}$  which cannot be obtained by competing methods.

**Acknowledgements** - This work was supported by the INL Laboratory Directed Research & Development (LDRD) Program under DOE Idaho Operations Office Contract DE-AC07-05ID14517. This research used resources of the National Energy Research Scientific Computing Center, a DOE Office of Science User Facility supported by the Office of Science of the U.S. Department of Energy under Contract No. DE-AC02-05CH11231.

[1] T. L. Gilbert, Phys. Rev. B **12**, 2111 (1975).

[2] R. A. Donnelly and R. G. Parr, Journal Of Chemical Physics **69**, 4431 (1978).

[3] M. Levy, Proceedings Of The National Academy Of Sciences Of The United States Of America **76**, 6062 (1979).

[4] M. Piris, in *Reduced-Density-Matrix Mechanics: with Application to Many-Electron Atoms and Molecules*, Vol. 134, edited by D. A. Mazziotti (John Wiley & Sons, 2007) p. 387.

[5] K. Pernal and K. J. Giesbertz, in *Density-Functional Methods for Excited States*, Vol. 368, edited by N. Ferre, M. Filatov, and M. Huix-Rotllant (Springer International Publishing Switzerland, 2016) pp. 125–184.

[6] W. Kutzelnigg, Journal Of Chemical Physics **40**, 3640 (1964).

[7] J. Cioslowski, K. Pernal, and M. Buchowiecki, Journal Of Chemical Physics **119**, 6443 (2003).

[8] M. Piris, X. Lopez, F. Ruiperez, J. M. Matxain, and J. M. Ugalde, Journal Of Chemical Physics **134**, 164102 (2011).

[9] K. Pernal, Computational And Theoretical Chemistry **1003**, 127 (2013).

[10] M. Piris and J. M. Ugalde, International Journal Of Quantum Chemistry **114**, 1169 (2014).

[11] R. Schade, E. Kamil, and P. Blochl, European Physical Journal-special Topics **226**, 2677 (2017).

[12] R. Lopez-Sandoval and G. M. Pastor, Phys. Rev. B **61**, 1764 (2000).

[13] R. Lopez-Sandoval and G. M. Pastor, Physical Review B **66**, 155118 (2002).

[14] R. Lopez-Sandoval and G. M. Pastor, Physical Review B **69**, 085101 (2004).

[15] M. Saubanere and G. M. Pastor, Phys. Rev. B **84**, 035111 (2011).

[16] W. Tows, M. Saubanere, and G. M. Pastor, Theoretical Chemistry Accounts **133**, 1422 (2013).

[17] E. Kamil, R. Schade, T. Pruschke, and P. E. Blochl, Phys. Rev. B **93**, 085141 (2016).

[18] M. Saubanere, M. B. Lepetit, and G. M. Pastor, Phys. Rev. B **94**, 045102 (2016).

[19] I. Mitxelena, M. Piris, and M. Rodriguez-Mayorga, Journal Of Physics-condensed Matter **29**, 425602 (2017).

[20] I. Mitxelena, M. Piris, and M. Rodriguez-Mayorga, Journal Of Physics-condensed Matter **30**, 089501 (2018).

[21] I. Mitxelena and M. Piris, Journal Of Chemical Physics **152**, 064108 (2020).

[22] I. Mitxelena and M. Piris, Journal of Physics: Condensed Matter **32**, 1701 (2020).

[23] N. Helbig, N. N. Lathiotakis, M. Albrecht, and E. Gross, Epl **77**, 67003 (2007).

[24] S. Sharma, J. K. Dewhurst, N. N. Lathiotakis, and E. Gross, Phys. Rev. B **78**, 201103 (2008).

[25] N. N. Lathiotakis, S. Sharma, J. K. Dewhurst, F. G. Eich, M. Marques, and E. Gross, Physical Review A **79**, 040501 (2009).

[26] S. Sharma, J. K. Dewhurst, S. Shallcross, and E. Gross, Phys. Rev. Lett. **110**, 116403 (2013).

[27] Y. Shinohara, S. Sharma, J. K. Dewhurst, S. Shallcross, N. N. Lathiotakis, and E. Gross, New Journal Of Physics **17**, 093038 (2015).

[28] P. Kent and G. Kotliar, Science **361**, 348 (2018).

[29] A. Georges, G. Kotliar, W. Krauth, and M. J. Rozenberg, Rev. Mod. Phys. **68**, 13 (1996).

[30] G. Kotliar and D. Vollhardt, Physics Today **57**, 53 (2004).

[31] G. Kotliar, S. Y. Savrasov, K. Haule, V. S. Oudovenko, O. Parcollet, and C. A. Marianetti, Rev. Mod. Phys. **78**,



- 865 (2006).
- [32] Z. Q. Cheng and C. A. Marianetti, Phys. Rev. Lett. **126**, 206402 (2021).
  - [33] Z. Q. Cheng and C. A. Marianetti, Phys. Rev. B **103**, 195138 (2021).
  - [34] Z. Cheng and C. Marianetti, Phys. Rev. B **106**, 205129 (2022).
  - [35] Z. Q. Cheng and C. A. Marianetti, Phys. Rev. B **108**, 035127 (2023).
  - [36] Z. Cheng and C. A. Marianetti, companion paper, Submitted to Phys. Rev. B.
  - [37] M. Chatziefleftheriou, A. Kowalski, M. Berovic, A. Amaricci, M. Capone, L. D. L. G. Sangiovanni, and L. de' Medici, Phys. Rev. Lett. **130**, 066401 (2023).
  - [38] A. Muller, Physics Letters A **105**, 446 (1984).
  - [39] G. Csanyi and T. A. Arias, Phys. Rev. B **61**, 7348 (2000).
  - [40] G. Csanyi, S. Goedecker, and T. A. Arias, Physical Review A **65**, 032510 (2002).
  - [41] R. Zitko and T. Pruschke, Phys. Rev. B **79**, 085106 (2009).
  - [42] M. Piris, Phys. Rev. Lett. **119**, 063002 (2017).
  - [43] H. Otsuka, J. Phys. Soc. Jpn. **61**, 1645 (1992).
  - [44] T. Yanagisawa, S. Koike, and K. Yamaji, J. Phys. Soc. Jpn. **67**, 3867 (1998).
  - [45] T. Yanagisawa, J. Phys. Soc. Jpn. **85**, 114707 (2016).
  - [46] T. Yanagisawa, J. Phys. Soc. Jpn. **88**, 054702 (2019).
  - [47] S. Sorella, Phys. Rev. B **107**, 115133 (2023).
  - [48] R. Levy, M. A. Morales, and S. W. Zhang, Physical Review Research **6**, 013237 (2024).
  - [49] T. Yanagisawa, M. Miyazaki, and K. Yamaji, Epl **134**, 27004 (2021).
  - [50] T. Yanagisawa, S. Koike, and K. Yamaji, Phys. Rev. B **64**, 184509 (2001).
  - [51] Y. X. Chen, L. F. Zhang, E. Weinan, and R. Car, Journal Of Chemical Theory And Computation **19**, 4484 (2023).
  - [52] J. P. Perdew, R. G. Parr, M. Levy, and J. L. Balduz, Phys. Rev. Lett. **49**, 1691 (1982).
  - [53] J. Bunemann and W. Weber, Phys. Rev. B **55**, 4011 (1997).
  - [54] H. Hasegawa, Journal of the Physical Society of Japan **66**, 1391 (1997).
  - [55] Y. Ono, M. Potthoff, and R. Bulla, Phys. Rev. B **67**, 035119 (2003).
  - [56] J. E. Han, M. Jarrell, and D. L. Cox, Phys. Rev. B **58**, 4199 (1998).
  - [57] T. Pruschke and R. Bulla, European Physical Journal B **44**, 217 (2005).
  - [58] L. de' Medici, Phys. Rev. B **83**, 205112 (2011).